Predicting the Efficiency of Corrugated Sheet Structured Packings with Large Specific Surface Area

Ž. Olujić, M. Behrens, L. Colli*, and A. Paglianti*
Laboratory for Process Equipment, Delft University of Technology, 2628 CA Delft, the Netherlands, e-mail: z.olujic@wbmt.tudelft.nl
*Department of Chemical Engineering, University of Pisa, 56126 Pisa, Italy

Original scientific paper
Received: December 5, 2003
Accepted: February 16, 2004

Dedicated to Prof. Egon Bauman

A thorough evaluation of the predictive accuracy of the Delft model has indicated that the predicted mass transfer efficiencies for vacuum and atmospheric conditions are too optimistic for packings with large specific surface areas, particularly those with a corrugation angle of 60 degrees. This occurred mainly due to an over-prediction of the effective interfacial area. To arrive at more conservative predictions in effective area, a well-known correlation for random packings was adapted to structured packing geometry. However this proved to be insufficient, and an additional correction factor expression was included to account explicitly for observed surface area and corrugation angle related effect. This resulted in a satisfactory accuracy over the whole range of packings and process conditions considered. Most importantly, with this addition the Delft model does not require any adjustable, packing specific parameter, and can be used to indicate optimal packing configuration for specific application needs.

Key words:
Effective area, structured packings, mass transfer efficiency, distillation

Introduction

Corrugated sheet structured packings are well-established and widely used gas/liquid contacting devices which proved to posses more potential for performance improvement than generally believed.[1] Of a great value in evaluating the hydraulic and mass transfer improvement potential was an overall predictive model, developed in parallel with a substantial experimental effort devoted to revealing the effects of variations in corrugation dimensions and physical properties.[2,3]

In the meantime, a consistent set of experimental, total reflux distillation test data has been used to validate thoroughly the predictive accuracy of the so called "Delft model" with respect to observed effects of the variations in the corrugation angles, specific surface area, surface design, and operating conditions. As reported by *Olujic* et al.[4] and *Fair* et al.,[5] the Delft model appeared to be too optimistic under vacuum and atmospheric conditions for packings with larger specific surface areas and generally predicts too small a difference in mass transfer efficiency resulting from the corrugation angle effect.

This paper describes the effort undertaken to alleviate in a practical manner the observed problems with the accuracy of the Delft model, which finally led to an overall predictive method that does not require any adjustable packing parameter.

Background

Here all working equations, used in conjunction with the Delft model, are presented correctly. Namely, in previous publications some vital expressions contain serious errors, such as Eq (31b) in a paper by *Olujic*[2] and Eq(43) in a paper by *Fair* et al.[5]

Packing geometry and flow related parameters

Outgoing data: α, ε, h, b, h_{pe}, n_{pe}, M_G, M_L, ρ_G, ρ_L, μ_G, μ_L, σ, D_G, D_L, and λ. In total reflux cases, the gas load factor, F_G, i.e. so called F-factor is readily available, and therefore it is more convenient to use in model calculations than the mass flow rates of phases.

Height of the packed bed:

$$h_{pb} = n_{pe} h_{pe} \tag{1}$$

Length of the triangular gas flow channel in a packing element:

$$l_{\mathrm{G,\,pe}} = \frac{h_{\mathrm{pe}}}{\sin\alpha} \tag{2}$$

Total length of the triangular zigzag gas flow channel in a packed bed:

$$l_{\mathrm{G,\,pb}} = n_{\mathrm{pe}} l_{\mathrm{G,pe}} = \frac{h_{\mathrm{pb}}}{\sin\alpha} \tag{3}$$

Corrugation side length:

$$s = \sqrt{\frac{b^2}{4} + h^2} \tag{4}$$

Installed specific surface area of packing:

$$a_{\mathrm{P}} = \frac{4s}{b\,h} \tag{5}$$

V-shaped fraction of the cross section of triangular gas flow channel occupied by liquid film:

$$\varphi = \frac{2s}{b + 2s} \tag{6}$$

Superficial gas and liquid velocities:

$$u_{\mathrm{Gs}} = \frac{4M_{\mathrm{G}}}{\rho_{\mathrm{G}}\,\pi\,d_{\mathrm{c}}^2} = \frac{F_{\mathrm{G}}}{\sqrt{\rho_{\mathrm{G}}}} \tag{7}$$

$$u_{\mathrm{Ls}} = \frac{4M_{\mathrm{L}}}{\rho_{\mathrm{L}}\,\pi\,d_{\mathrm{c}}^2} \tag{8a}$$

For total reflux (L/V = 1) conditions:

$$\mu_{\mathrm{Ls}} = u_{\mathrm{Gs}}\frac{\rho_{\mathrm{G}}}{\rho_{\mathrm{L}}} \tag{8b}$$

The effective liquid flow angle:

$$\alpha_{\mathrm{L}} = \arctan\left[\frac{\cos(90-\alpha)}{\sin(90-\alpha)\cos\left[\arctan\left(\frac{b}{2h}\right)\right]}\right] \tag{9}$$

The mean liquid film thickness:

$$\delta = \left(\frac{3\mu_{\mathrm{L}}u_{\mathrm{Ls}}}{\rho_{\mathrm{L}}g\,a_{\mathrm{p}}\sin\alpha_{\mathrm{L}}}\right)^{\frac{1}{3}} \tag{10}$$

Liquid hold-up:

$$h_{\mathrm{L}} = \delta\cdot a_{\mathrm{p}} \tag{11}$$

Hydraulic diameter of triangular gas flow channel:

$$d_{\mathrm{hG}} = \frac{\frac{(bh-2\delta s)^2}{bh}}{\left[\left(\frac{bh-2\delta s}{2h}\right)^2 + \left(\frac{bh-2\delta s}{b}\right)^2\right]^{0.5} + \frac{bh-2\delta s}{2h}} \tag{12}$$

For $\delta = 0$ (dry bed) hydraulic diameter expression reduces to:

$$d_{\mathrm{hG,\,dry}} = \frac{2bh}{b+2s} \tag{13}$$

Effective gas and liquid velocities:

$$u_{\mathrm{Ge}} = \frac{u_{\mathrm{Gs}}}{(\varepsilon - h_{\mathrm{L}})\sin\alpha} \tag{14}$$

$$u_{\mathrm{Le}} = \frac{u_{\mathrm{Ls}}}{\varepsilon\,h_{\mathrm{L}}\sin\alpha_{\mathrm{L}}} \tag{15}$$

Effective and relative velocity based Reynolds numbers:

$$\mathrm{Re}_{\mathrm{Ge}} = \frac{\rho_{\mathrm{G}}u_{\mathrm{Ge}}d_{\mathrm{hG}}}{\mu_{\mathrm{G}}} \tag{16}$$

$$\mathrm{Re}_{\mathrm{Grv}} = \frac{\rho_{\mathrm{G}}(u_{\mathrm{Ge}} + u_{\mathrm{Le}})\,d_{\mathrm{hG}}}{\mu_{\mathrm{G}}} \tag{17}$$

Pressure drop model equations

Full operating range:

$$\left(\frac{\Delta p}{\Delta z}\right) = \left(\frac{\Delta p}{\Delta z}\right)_{\mathrm{preload}} F_{\mathrm{load}} \tag{18}$$

Pressure drop enhancement factor for the loading region:

$$F_{\mathrm{load}} = 3.8\left(\frac{F_{\mathrm{G}}}{F_{\mathrm{G,lp}}}\right)^{\frac{2}{\sin\alpha}}\left(\frac{u_{\mathrm{Ls}}^2}{\varepsilon^2 g\,d_{\mathrm{hG}}}\right)^{0.13} \tag{19}$$

Loading point F-factor, i.e. the point of departure from preloading conditions:

Form suitable for total reflux conditions (L/V = 1):

$$F_{\mathrm{G,lp}} = \left(0.053\,\varepsilon^2 g\,d_{\mathrm{hG}}(\rho_{\mathrm{L}}-\rho_{\mathrm{G}})\left(\frac{u_{\mathrm{Ls}}}{u_{\mathrm{Gs}}}\sqrt{\frac{\rho_{\mathrm{L}}}{\rho_{\mathrm{G}}}}\right)^{-0.25}(\sin\alpha)^{1.15}\right)^{0.5} \tag{20a}$$

Form suitable for constant liquid load (L/V ≠ 1) case:

$$F_{\mathrm{G,lp}} = \left(0.053\,\varepsilon^2 g\, d_{\mathrm{hG}} \left(\frac{\rho_{\mathrm{L}}-\rho_{\mathrm{G}}}{\rho_{\mathrm{G}}}\right)\cdot\right.$$
$$\left.\cdot\left(u_{\mathrm{Ls}}\sqrt{\frac{\rho_{\mathrm{L}}}{\rho_{\mathrm{G}}}}\right)^{-0.25}(\sin\alpha)^{1.24}\right)^{0.57}\sqrt{\rho_{\mathrm{G}}} \quad (20b)$$

By multiplying the right hand side of these expressions with 0.9 a safer value is obtained.

Preloading region pressure drop:

$$\Delta p_{\mathrm{preload}} = \Delta p_{\mathrm{GL}} + \Delta p_{\mathrm{GG}} + \Delta p_{\mathrm{DC}} =$$
$$= (s_{\mathrm{GL}} + s_{\mathrm{GG}} + s_{\mathrm{DC}})\frac{\rho_{\mathrm{G}} u_{\mathrm{Ge}}^2}{2} \quad (21)$$

Overall gas/liquid interaction coefficient:

$$\zeta_{\mathrm{GL}} = \varphi\,\xi_{\mathrm{GL}}\frac{h_{\mathrm{pb}}}{d_{\mathrm{hG}}\sin\alpha} \quad (22)$$

Gas/liquid friction factor:

$$\xi_{\mathrm{GL}} = \left\{-2\log\left[\frac{(\delta/d_{\mathrm{hG}})}{3.7} - \frac{5.02}{\mathrm{Re}_{\mathrm{Grv}}}\log\left(\frac{(\delta/d_{\mathrm{hG}})}{3.7} + \frac{14.5}{\mathrm{Re}_{\mathrm{Grv}}}\right)\right]\right\}^{-2} \quad (23)$$

Gas/gas interaction coefficient:

$$\zeta_{\mathrm{GG}} = (1-\varphi)\,\xi_{\mathrm{GG}}\frac{h_{\mathrm{pb}}}{d_{\mathrm{hG}}\sin\alpha} =$$
$$= (1-\varphi)\,0.722\,(\cos\alpha)^{3.14}\frac{h_{\mathrm{pb}}}{d_{\mathrm{hG}}\sin\alpha} \quad (24)$$

Direction change losses coefficient:

$$\zeta_{\mathrm{DC}} = \frac{h_{\mathrm{pb}}}{h_{\mathrm{pe}}}(\xi_{\mathrm{bulk}} + \psi\,\xi_{\mathrm{wall}}) \quad (25)$$

with

$$\psi = \frac{2h_{\mathrm{pe}}}{\pi\, d_{\mathrm{c}}^2\tan\alpha}\left(d_{\mathrm{c}}^2 - \frac{h_{\mathrm{pe}}^2}{\tan^2\alpha}\right)^{0.5} +$$
$$+\frac{2}{\pi}\arcsin\left(\frac{h_{\mathrm{pe}}}{d_{\mathrm{c}}\tan\alpha}\right) \quad (26)$$

$$\xi_{\mathrm{bulk}} = 1.76\,(\cos\alpha)^{1.63} \quad (27)$$

$$\xi_{\mathrm{wall}} = \frac{4092\,u_{\mathrm{Ls}}^{0.31} + 4715(\cos\alpha)^{0.445}}{\mathrm{Re}_{\mathrm{Ge}}} +$$
$$+34.19\,u_{\mathrm{Ls}}^{0.44}(\cos\alpha)^{0.779} \quad (28)$$

Mass transfer model equations

Overall, Height Equivalent to Theoretical Plate (HETP) expressions:

$$\mathrm{HETP} = \left[\frac{\ln\lambda}{\lambda-1}\right]\mathrm{HTU}_{\mathrm{Go}} \quad (29)$$

$$\mathrm{HTU}_{\mathrm{Go}} = \mathrm{HTU}_{\mathrm{G}} + \lambda\,\mathrm{HTU}_{\mathrm{L}} \quad (30)$$

$$\mathrm{HTU}_{\mathrm{G}} = \frac{u_{\mathrm{Gs}}}{k_{\mathrm{G}}a_{\mathrm{e}}} \quad (31)$$

$$\mathrm{HTU}_{\mathrm{L}} = \frac{u_{\mathrm{Ls}}}{k_{\mathrm{L}}a_{\mathrm{e}}} \quad (32)$$

Stripping factor:

$$\lambda = \frac{m}{(L/V)} = \frac{\alpha_{\mathrm{lk}}}{[1+(\alpha_{\mathrm{lk}}-1)x_{\mathrm{lk}}]^2}\left(\frac{V}{L}\right) \quad (33)$$

Gas phase mass transfer coefficient:

$$k_{\mathrm{G}} = \sqrt{k_{\mathrm{G,lam}}^2 + k_{\mathrm{G,turb}}^2} \quad (34)$$

with

$$k_{\mathrm{G,lam}} = \frac{Sh_{\mathrm{G,lam}}D_{\mathrm{G}}}{d_{\mathrm{hG}}} \quad (35)$$

$$k_{\mathrm{G,turb}} = \frac{Sh_{\mathrm{G,turb}}D_{\mathrm{G}}}{d_{\mathrm{hG}}} \quad (36)$$

$$Sh_{\mathrm{G,lam}} = 0.664\,Sc_{\mathrm{G}}^{1/3}\sqrt{\mathrm{Re}_{\mathrm{Gvr}}\frac{d_{\mathrm{hG}}}{l_{\mathrm{G,pe}}}} \quad (37)$$

$$Sh_{\mathrm{G,turb}} = \frac{\mathrm{Re}_{\mathrm{Grv}}\,Sc_{\mathrm{G}}\,\frac{\xi_{\mathrm{GL}}\varphi}{8}}{1+1.27\sqrt{\frac{\xi_{\mathrm{GL}}\varphi}{8}}\,(Sc_{\mathrm{G}}^{2/3}-1)}\left[1+\left(\frac{d_{\mathrm{hG}}}{l_{\mathrm{G,pe}}}\right)^{2/3}\right] \quad (38)$$

$$Sc_{\mathrm{G}} = \frac{\mu_{\mathrm{G}}}{\rho_{\mathrm{G}}D_{\mathrm{G}}} \quad (39)$$

Liquid phase mass transfer coefficient:

$$k_{\mathrm{L}} = 2\sqrt{\frac{D_{\mathrm{L}}u_{\mathrm{Le}}}{\pi\,0.9\,d_{\mathrm{hG}}}} \quad (40)$$

Effective (interfacial) area equations

As demonstrated in a recent paper by *Fair* et al.[5], by incorporating the original *Onda* et al.[6] correlation for predicting the effective area of structured packings, the Delft model does not require any packing specific empirical parameter. It however makes a distinction between unperforated and perforated packings, by adopting following expression for the effective area:

$$a_e = (1-\Omega)\, a_{e,Onda} = (1-\Omega)\, a_p \cdot \cdot \left\{1 - \exp\left[-1.45\left(\frac{0.075}{\sigma}\right)^{0.75} \mathrm{Re}_L^{0.1}\, Fr_L^{-0.05}\, We_L^{0.2}\right]\right\} \quad (41)$$

where Ω (–) represents the fraction of packing surface area occupied by holes, a_p (m^{-1}) is the installed, specific surface area, and the expression in the brackets represents the well known *Onda* correlation,[6] with characteristic dimensionless Reynolds, Weber and Froude numbers, respectively, defined as

$$\mathrm{Re}_L = \frac{\rho_L u_{Ls}}{a_p \mu_L} \quad (42)$$

$$We_L = \frac{\rho_L u_{Ls}^2}{a_p \sigma} \quad (43)$$

$$Fr_L = \frac{u_{Ls}^2 a_p}{g} \quad (44)$$

where σ (N/m) is the surface tension of liquid, μ_L (Pa s) is the dynamic viscosity of liquid, ρ_L (kg/m^3) is the density of liquid, and g (m/s^2) is gravity acceleration.

For unperforated packings, such as Montz B1 series, $\Omega = 0$, and for packings with common size and pattern of holes (around 4 mm), such as Montz BSH, Koch-Glitsch Flexipac, and Sulzer Mellapak packings, the void fraction of the surface area is around 10 % ($\Omega = 0.1$). In other words, with this it is assumed that the perforated packings have roughly 10 % less installed area for the same specific surface area. This may be so in case of low surface tension liquids in conjunction with low liquid loads. It is less probable in aqueous systems, because at moderate and high liquid loads, as encountered in near atmospheric applications, the high surface tension liquid will tend to bridge the holes and thus effectively increase the interfacial area.

With the specific surface area of the structured packing as the linear dimension in characteristic dimensionless numbers, the correlation by *Onda* et al.[6] allows for a more pronounced pressure effect and consequently ensures more conservative efficiency predictions than the original empirical correlation used previously in conjunction with the Delft model.

Interestingly, the hydraulic diameter of gas as linear dimension in the above equations produces identical values as the original empirical one. Using the corrugation side and hydraulic diameter of the liquid phase results in respectively too high and too low values[5], which, if implemented, affect adversely the overall predictive accuracy of the Delft model.

A thorough evaluation of the predictive accuracy of the Delft model[5,7] indicated that predictions are too optimistic with regard to measured values for structured packings with specific surface area of around 400 m^2/m^3. Since the trends in efficiency curves appeared to be correct, the overestimated interfacial area was considered as the wrongdoer in this case.

In earlier studies it was assumed that the wetting behaviour of certain packing would be independent of the size of specific surface area, i.e. the size of corrugations. However, from the experience it is known that larger specific area packings use less effectively the installed area than the common size packings.[3,8] This may be mainly attributed to the fact that with the increasing number of corrugations, i.e. flow channels, particularly those with sharper corrugation ridges, the liquid will experience more difficulties in its tendency to spread laterally. A thorough discussion of experimental and modelling issues related to determination of effective surface area of corrugated sheet structured packings can be found elsewhere.[4,9]

Model evaluation

The experimental data used in this study for model evaluation are the total reflux distillation data obtained with a number of J. Montz packings using the 0.43 m ID column available at the Separations Research Program (SRP) of the University of Texas at Austin. All experiments have been performed with cyclohexane/n-heptane system at operating pressures ranging from 0.33 to 4.14 bar using a high performance narrow trough distributor comprising 145 drip points per square meter.

Packings considered in this study are B1-250.60, B1-400, B1-400.60, BSH-400, and BSH-400.60. Numbers 250 and 400 stand for the nominal specific surface area in m^2/m^3. It should be noted that actual areas differ to some extent from the nominal ones. Extension "60" indicates packings with a corrugation inclination angle of 60 degrees with horizontal. B1 is well-known Montz packing with shallow embossed, unperforated surface, while BSH packing is made of expanded metal and contains a regular pattern of holes. The experimental set-up, the test system and the packings tested, including all macro geometry dimensions, have been thoroughly described elsewhere.[3]

Figure 1 shows predicted effective surface area for B1-400.60 packing as a function of F-factor and the operating pressure, as calculated using Eq(41). Also original curves are added to illustrate the dif-

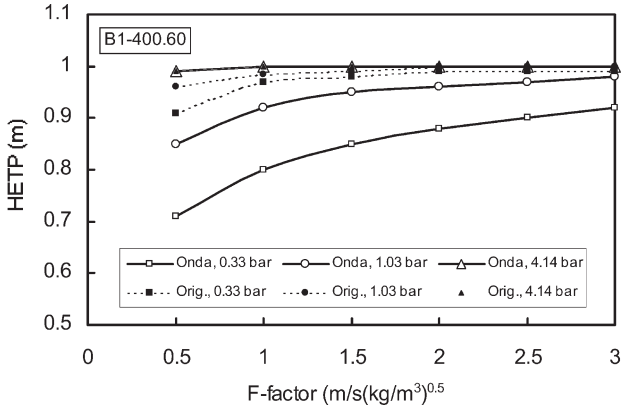

F i g . 1 – *Comparison of predicted effective areas*

ference. It should be noted that with both increasing operating pressure and, for a given pressure, increasing F-factor (total reflux) the liquid load increases proportionally to the gas load and the ratio of vapour and liquid densities. In case of original, empirical correlation these effects are practically negligible. Although the Eq(41) assumes a considerable loss of effective area at F-factors below 1, particularly at vacuum conditions, the effect on mass transfer efficiency is nearly negligible, as illustrated in case of predicted B1-400.60 curves shown in Figure 2. The experimental curve lies well above predicted ones, and this is also the case with B1-400 packing however to a lesser extent. On the other hand, the agreement between experiment and prediction for B1-250.60 packing is very well. One should note that the Delft model was developed for preloading range only, and does not account implicitly for complex phenomena observed in the loading range, which, according to Figure 2, can lead to opposite effects, i.e. improvement (60° packings) or deterioration (B1-400) in the performance. However, these effects are difficult to describe, and there is no practical need for this, because the extension of preloading curve into loading range ensures conservative enough predictions around the design point, say at 80 % of the flooding limit.

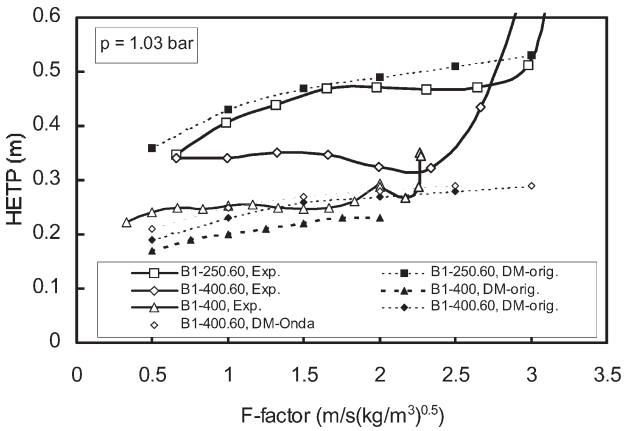

F i g . 2 – *Predictive accuracy with the original and the Eq(41) for effective area*

Figure 3 shows the effect of the operating pressure, i.e. the liquid load on the performance of expanded metal packing BSH-400.60. All calculated efficiency curves have been obtained using Eq(41), which means a slightly closer approach to experimental ones than with the original empirical correlation for effective area. The deviation from experiment is still large, and is more pronounced at vacuum and the atmospheric pressure. Strikingly, in case of BSH-400 packing (45° corrugation angle), the agreement between experiment and prediction is nearly ideal.

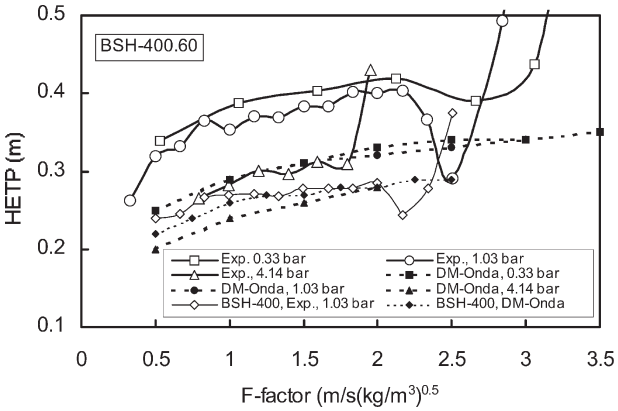

F i g . 3 – *Performance of expanded metal packings, measured vs. predicted, using Eq(41)*

In contrast to B1-400, BSH-400 at atmospheric pressure exhibited a significant improvement in the efficiency beyond the loading point, which is astonishingly large in case of 60° (BSH-400.60) packing. In general, at highest operating pressure encountered in this study, 4.14 bar (with liquid loads well above 40 m^3/m^2h) there is no improvement in the efficiency, rather a steady deterioration exploding upon reaching the onset of flooding. Certainly, it is not only the effective area affected strongly by violent interaction of phases in the loading range, particularly at the interfaces between packing elements, but also the kinetics of mass transfer as well as the driving forces. However, this is too complex to be described in a fundamental way, and the designers of packed columns avoid generally dealing with the loading range phenomena by adding sufficient safety factors to preloading range values predicted usually by a purely empirical method.

Certainly the exhibited accuracy in case of common size packings is more than satisfactory, and for larger surface area packings the predictions are still too optimistic for vacuum and atmospheric pressure, particularly for 60 degrees packings. Obviously, the challenge here is to improve the accu-

racy of the model on the large specific surface area side and for the large corrugation angle, without affecting adversely the accuracy experienced with common size/angle packings.

Model improvement considerations

Although there is no strong interaction between phases in the preloading range, the relationship between effective area, geometrical features of packing, physical properties of the system, and operating conditions is very complex, and not yet understood good enough to enable development of a purely fundamental model. So we need to proceed along the well-established empirical approach to arrive at a predictive model that will enable a closer approach to reality.

In general, Eq(41) contains already all relevant dimensionless numbers and could hardly be improved from inside to account for such a loss of surface area as experienced in our studies with both large surface area and corrugation angle packings. Therefore, the observed excessive loss of effective area is accounted for by adopting an empirical correction term, added to right hand side of Eq(41).[10]

$$a_e = a_{e,Eq(41)} \left(\frac{\sin 45°}{\sin \alpha_L} \right)^n \qquad (41a)$$

where α_L (°) is the effective angle of the liquid flow, described by Eq(9), and the exponent n accounts for the effects of other relevant factors.

According to the theoretically derived Eq(9), the liquid driven by gravity will flow under an effective angle larger than the corrugation angle, which affects the efficiency adversely, but not in a strong manner. Presence of the apertures in the surface such as holes and other shapes, particularly those slit-like could force liquid to leave a channel and go to the other side of the sheet, i.e. to flow under an effective angle steeper than that of an unperforated packing. This becomes more probable with decreasing surface tension and generally it is more pronounced at low liquid loads. Water, which is mostly encountered in near atmospheric applications is capable of bridging over the common size holes, which implies that with water the above equation may be more or less valid also for packings with perforations such as BSH, Flexipac and Mellapak.

Surface area reduction related effects are lumped together with other governing variables in an empirical expression for the exponent n in the correction term on the right hand side of Eq(41a). Here, the common size, specific surface area of 250 m^2/m^3, the corrugation angle of 45° and the atmospheric pressure are taken as reference points. The working, empirical expression for n is

$$n = \left(1 - \frac{a_p}{250}\right)\left(1 - \frac{\alpha_L}{45}\right) + \ln\left(\frac{a_{e,Onda}}{250}\right) + \left(0.49 - \sqrt{\frac{1.013}{p_{op}}}\right)\left(1.2 - \frac{\alpha_L}{45}\right) \qquad (45)$$

where p_{op} (bar) is the operating pressure.

Effectively, the correction term on the right hand side of Eq(41a) with the exponent n described by the above expression, reduces the size of effective area predicted by Eq(41), to the extent corresponding to the observed effects.

Results and discussion

Figure 4 shows the situation from the Figure 2, now with efficiency curves calculated using the Eq(41a) in conjunction with the Eq(45). Obviously, a much better accuracy is obtained for large surface area packings than before. The predictions deviate appreciably from the experiment in the lower region of F-factors, but match fairly well with the experiment around the design/loading point.

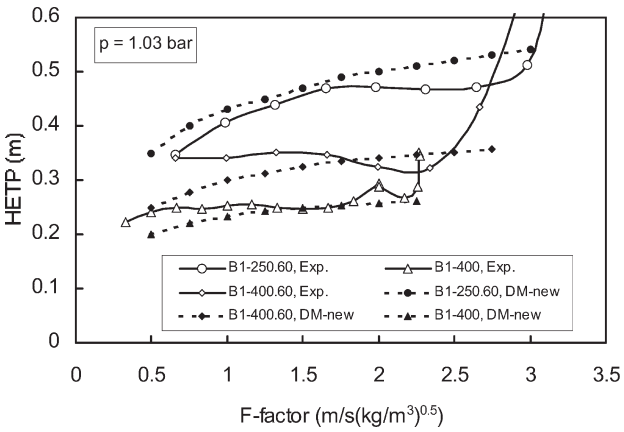

Fig. 4 – *Performance of sheet metal packings, measured vs. predicted, using Eq(41a)*

Figure 5 shows the comparison of experimental and predicted curves for B1-400.60, at three different operating pressures. Here, the deviation from the experiment is still considerable in lower F-factor region for atmospheric and the vacuum condition case. Certainly, this is due to a correspondingly low liquid load, and the related difficulties in the spreading of liquid over the corrugations of this size of B1 series packing. At relatively low liquid loads (low F-factor), the sharp corrugation ridges and unperforated surface force the liquid to follow the

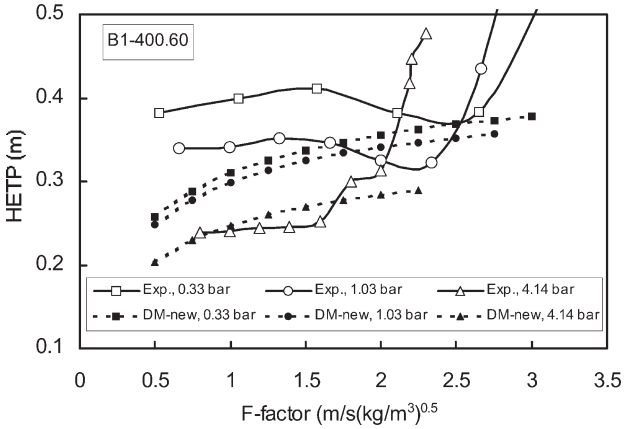

Fig. 5 – *Effect of the operating pressure on the performance of sheet metal (B1 series) packing, measured vs. predicted, using Eq(41a)*

channel. At higher F-factors, the liquid is forced by the vapour flow to mix thoroughly and spread laterally at transitions between packing elements. This improves substantially the active wetting and consequently the performance of packing. Because of the design of corrugated sheets, the effect of operating pressure/liquid load is much more pronounced in case of B1-400.60 packing than in the case of similar 60° BSH packing (see Figure 6). The performance of the later one is predicted with an astonishingly good accuracy, and this is reached, as illustrated in Figure 6, without bringing any damage to the accuracy in case of BSH-400 packing.

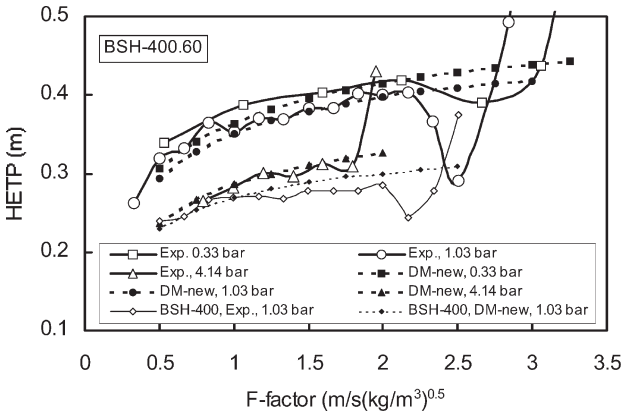

Fig. 6 – *Effect of the operating pressure on the performance of expanded metal (BSH series) packing, measured vs. predicted, using Eq(41a)*

Conclusions

The Delft model described in detail here proved to be a versatile conceptual design tool for columns containing structured packings. With the proposed empirical extension of the *Onda* et al. correlation for the effective area, the Delft model enables also a fairly accurate prediction of the mass transfer efficiency of larger specific surface area packings, employed in separations of fine chemicals and cryogenic distillation of air. More importantly, it does not require any adjustable parameter to predict reliably the effect of geometry on the mass transfer performance of corrugated sheet structured packings in the wide range of process conditions. As such it may be used to tailor the packings to specific needs.

ACKNOWLEDGEMENT

Authors wish to thank the Julius Montz GmbH for the permission to use the original test data.

Nomenclature

a_e – effective (interfacial) area, m^2/m^3
a_p – specific surface area of packing, m^2/m^3
b – corrugation base length, m
D_G – gas phase diffusion coefficient, m^2/s
D_L – liquid phase diffusion coefficient, m^2/s
d_c – column diameter, m
d_{hG} – hydraulic diameter for the gas phase, m
F_G – $u_{Gs}(\rho_G)^{0.5}$ = gas load factor, m/s $(kg/m^3)^{0.5}$
$F_{G,lp}$ – loading point gas load factor, m/s $(kg/m^3)^{0.5}$
F_{load} – loading effect factor, –
Fr_L – Froude number for the liquid, –
g – gravity acceleration, m/s^2
$HETP$ – height equivalent to a theoretical plate, m
HTU_G – height of a gas phase transfer unit, m
HTU_L – height of a liquid phase transfer unit, m
HTU_{Go} – height of an overall gas phase related transfer unit, m
h – corrugation height, m
h_L – operating liquid hold up, – (m^3 liquid/m^3 bed)
h_{pb} – height of the packed bed, m
h_{pe} – height of the packing element, m
k_G – gas phase mass transfer coefficient, m/s
k_L – liquid phase mass transfer coefficient, m/s
L – molar flow rate of liquid, kmol/s
$l_{G,pb}$ – total length of gas flow channel in a packed bed, m
$l_{G,pe}$ – length of gas flow channel in a packing element, m
M_G – mass flow rate of gas/vapor, kg/s
M_L – mass flow rate of liquid, kg/s
m – slope of the equilibrium line, –
n – exponent in Eq. (41), –
n_{pe} – number of packing elements (layers) in a bed, –
p, p_{op} – operating pressure, bar
Re_{Ge} – effective gas phase Reynolds number, –
Re_{Grv} – relative velocity Reynolds number, –
Re_L – Reynolds number for the liquid, –

Sc_G – Schmidt number for gas, –
Sh_G – Sherwood number for gas, –
s – corrugation side length, m
u_{Ge} – effective gas velocity, m/s
u_{Gs} – superficial gas velocity, m/s
u_{Le} – effective liquid velocity, m/s
u_{Ls} – superficial liquid velocity, m/s
V – molar flow rate of vapor, kmol/s
We_L – Weber number for the liquid, –
x_{lk} – mole fraction of the light component in liquid phase, –

Greek letters

α – corrugation inclination angle, ^{0}
α_L – effective liquid flow angle, ^{0}
α_{lk} – relative volatility of the light component, –
δ – liquid film thickness, m
ε – packing porosity, m^3 voids/m^3 bed
φ – fraction of the triangular flow channel occupied by liquid, –
μ_G – viscosity of gas, Pa s
μ_L – viscosity of liquid, Pa s
λ – m/(L/V) = stripping factor, –
ρ_G – density of gas, kg/m^3
ρ_L – density of liquid, kg/m^3
σ – surface tension, N/m
ζ_{DC} – overall coefficient for direction change losses, –
ζ_{GG} – overall coefficient for gas-gas friction losses, –
ζ_{GL} – overall coefficient for gas-liquid friction losses, –
ξ_{bulk} – direction change factor for bulk zone, –
ξ_{GG} – gas-gas friction factor, –
ξ_{GL} – gas-liquid friction factor, –
ξ_{wall} – direction change factor for wall zone, –
Ω – fraction of packing surface area occupied by holes, –
ψ – fraction of gas flow channels ending at column walls, –

Subscripts

G – gas or vapor
L – liquid
lam – laminar flow
turb – turbulent flow

References

1. *Olujic, Z., Jansen, H., Kaibel, B., Rietfort, T., Zich, E.,* Stretching the Capacity of Structured Packings, Ind. Eng. Chem. Res. **40** (2001) 6172.
2. *Olujic, Z.,* Development of a Complete Simulation Model for Predicting the Hydraulic¸and Separation Performance of Distillation Columns Equipped with Structured Packings, Chem. Biochem. Eng. Q. **11** (1997) 31.
3. *Olujic, Z., Seibert, A. F., Fair, J. R.,* Influence of Corrugation Geometry on the Performance of Structured Packings: An Experimental Study, Chem. Eng. Processing **39** (2000) 335.
4. *Olujic, Z., Kamerbeek, A.B., de Graauw, J.,* A Corrugation Geometry Based Model for Efficiency of Structured Distillation Packing, Chem. Eng. Processing **38** (1999) 683.
5. *Fair, J. R., Seibert, A. F., Behrens, M., Saraber, P. P., Olujic, Z.,* Structured Packing Performance – Experimental Evaluation of Two Predictive Models, Ind. Eng. Chem. Res. **39** (2000) 1788.
6. *Onda, K.; Takeuchi, H.; Okumoto, Y.,* Mass Transfer Coefficients Between Gas and Liquid Phases in Packed Columns, J. Chem. Eng. Japan **1** (1968) 56.
7. *Colli, L.*, A Fluidynamic Study of Structured Packings for Vacuum Distillation Applications, MSc. Thesis (tesa di laurea), University of Pisa, Pisa, Italy, February 2000.
8. *Olujic, Z., Seibert, A. F.; Kaibel, B.; Jansen, H.; Rietfort, T.; Zich, E.,* Performance characteristics of a new high capacity structured packing, Chem. Eng. Processing **42** (2003) 55.
9. *Brunazzi, E.; Nardini, G.; Paglianti, A.; Petarca, L.,* Interfacial Area of Mellapak Packing: Absorption of 1,1,1-Trichloroethane by Genosorb 300, Chem. Eng. Technol. **18** (1995) 248.
10. *Colli, L., Paglianti, A., Behrens, M., Olujic, Z.,* Predicting the Effect of the Corrugation Angle on Mass Transfer Performance of Structured Packings with Larger Surface Area, Paper (Poster) presented at the 5th Italian Conference on Chemical and Process Engineering (ICheaP 5), 20–23 May, 2001, Florence, Italy.